

Boundary Conditions in Head Injury  
Finite Element Modeling

Catherine G. Galbraith and Pin Tong

US Department of Transportation  
Transportation Systems Center  
DTS 76, Kendall Square, Cambridge, MA 02142

**ABSTRACT**

A three dimensional finite element model (FEM) of a simplified coronal cross section of a head was built to simulate diffuse axonal injury (DAI) physical model (PM) experiments which were performed at the University of Pennsylvania (Penn). The purpose of this study was to investigate the effect of boundary conditions on brain displacement and strain.

The PMs that were used in this study are aluminum half cylinders filled with a transparent silicone gel which contains an imbedded orthogonal grid. The models were subjected to a non-centroidal rotation, and the resulting grid deformations were recorded.

In the FEMs, the brain was modeled as a three element linear viscoelastic solid, and the skull was modeled as a nearly rigid half cylinder. The material constants were chosen so that the initial shear modulus corresponded to the value of Young's modulus reported by Penn with a Poisson's ratio of 0.499.

The FEMs were subjected to the same loading as the PMs, and updated Lagrangian coordinates were used to permit large deformations and rotations of the surrogate brain. They were designed with not only the pure slip and no slip interfaces between the skull that are present in the PM but also, with several coefficients of friction.

Comparison of the x and y displacements of the boundary nodes of the slip and no slip physical and finite element models shows a large difference between the boundary conditions in the FEMs but little difference in the PMs. Closer examination of the PMs reveals that they are neither pure slip or no slip at the boundaries.

When the PM x and y displacements of various nodes are compared with those from FEMs having varying amounts of friction in the brain-skull interface, it is shown that both the slip and no slip PMs are best approximated by a FEM with a 0.05 coefficient of friction in the interface.

Analysis of the maximum principal strain in the finite element simulations illustrates the influence of boundary condition on contour patterns, maximum strain values, and time history of strain. These results indicate the importance of determining the appropriate boundary condition for future modeling efforts.

## INTRODUCTION

The objective of this study is to investigate the effects of the brain-skull boundary condition on brain deformation and principal strain location during non-impact head injury. This has been done through the use of a finite element simulation of physical model (PM) experiments performed by the University of Pennsylvania (Penn). [1,2] The PMs that were used in this series of simulations are aluminum half-cylinders filled with a silicone gel in which an orthogonal grid was imbedded.

During the experiment, these models were mounted to a linkage on a HYGE™ piston and subjected to approximately 65° of rotation. The tangential acceleration of this motion is shown in Figure 1. The resulting grid deformation was digitized from high speed film recordings and stored. This data was used for validation of the finite element model (FEM).

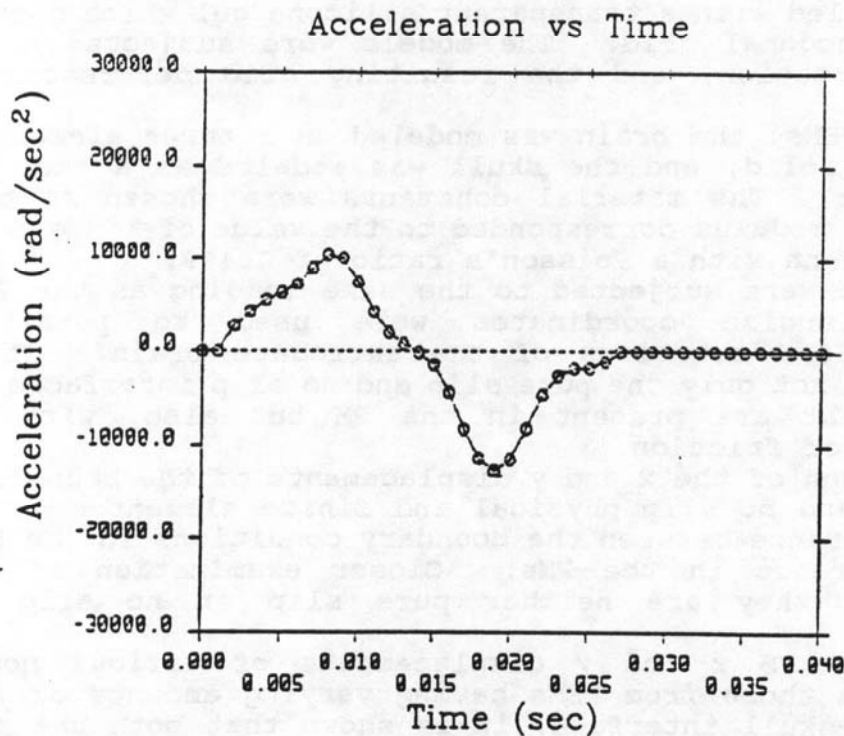


Figure 1: Tangential Acceleration vs Time

## MATERIALS AND METHODS

The FEM was developed through the use of the INGRID, DYNA3D, and TAURUS finite element package [3]. The three dimensional model is zoned similarly to the PM, and it is composed of a nearly rigid shell and a viscoelastic interior. (See Figure 2). The constitutive equation and material constants of the interior are shown in Figure 3. The constants were chosen so that the initial shear modulus corresponded to the value of Young's modulus reported by Penn with a Poisson's ratio of 0.499, and the time constant was chosen to yield maximum damping.

Since the boundary condition between the interior and the shell was reported to be either pure slip or pure no slip in the PM, two FEMs were constructed - one with each of the boundary conditions.

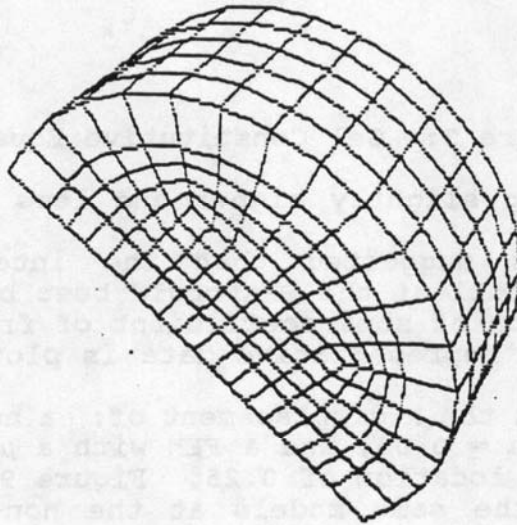


Figure 2: Finite Element Model Grid

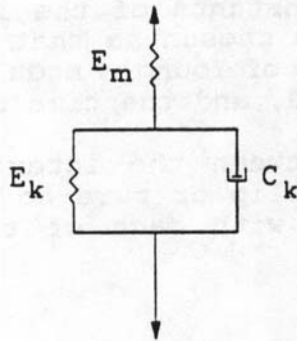
## RESULTS

### Comparison of the Physical and Finite Element Models

The FEM was subjected to the same load time history as the PM, and a comparison of the displacement of grid nodes at non-dimensional radial locations of 0 and 1 in x and y directions for the no slip PM and FEM are shown in Figures 4 and 5. These results show that while the FEM does not move at these nodes, the PM does. The x and y displacements at the same radial locations for the slip physical and finite element models are shown in Figures 6 and 7. These figures show a different result, the displacements of the FEM are greater than those of the PM. However, the magnitudes of the displacements in the slip and no slip physical models are approximately equal, with the slip PM

### Constitutive Equation

$$G(t) = G_{\infty} + (G_0 - G_{\infty}) e^{-\beta t}$$



$$G_{\infty} = \frac{E_m \cdot E_k}{E_m + E_k} = 0.8 \text{ psi}$$

$$G_0 = E_m = 1.6 \text{ psi}$$

$$\beta = \frac{E_m + E_k}{C_k} = 200 \text{ sec}^{-1}$$

Figure 3: Gel Constitutive Equation

displacements being slightly higher and less than half of those for the slip FEM.

These results suggested that the interface between the interior and the shell of the PMs could best be approximated with a boundary condition of some coefficient of friction. This was done and, representative data is plotted in Figures 8 - 11.

Figure 8 shows the x displacement of: a no slip PM, a no slip FEM, a FEM with a  $\mu = 0.05$ , and a FEM with a  $\mu = 0.25$  at the non-dimensional radial location of 0.25. Figure 9 is a plot of the x displacement for the same models at the non-dimensional radial location of 0.75.

The data in Figure 10 shows the x displacement of: a slip PM, a slip FEM, a FEM with a  $\mu = 0.05$ , and a FEM with a  $\mu = 0.25$  at the non-dimensional location of 0.25. Figure 11 is a plot of the x displacement for the same models at the non-dimensional radial location of 0.75.

Figures 8 - 11 show that the slip and no slip PMs are bounded by the FEM simulations. The PM x displacements at various non-dimensional radial locations agree best with a FEM which has a coefficient of friction equal to 0.05 in the interior - shell interface.

#### Strain Contours of the Slip and No Slip Finite Element Models

Figures 12 - 19 are strain contours for the slip and no slip FEMs at every 10 msec during the simulation. In comparing the two boundary conditions, it can be seen that the maximum strain

No Slip Physical and Finite Element X Boundary  
Displacement vs Time

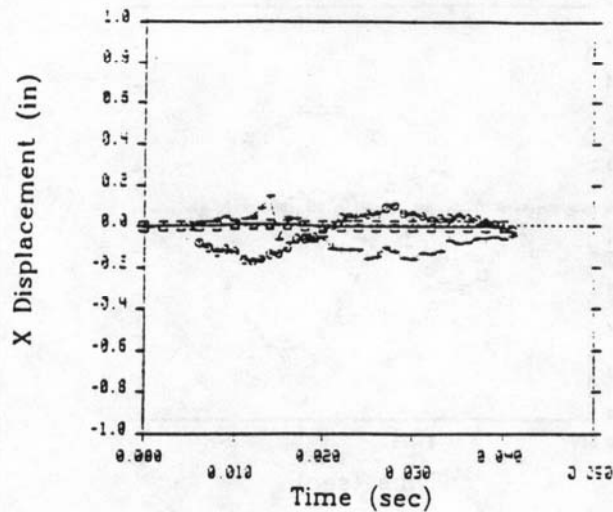


Figure 4: No Slip Physical and Finite Element  
X Boundary Displacement vs Time

No Slip Physical and Finite Element Y Boundary  
Displacement vs Time

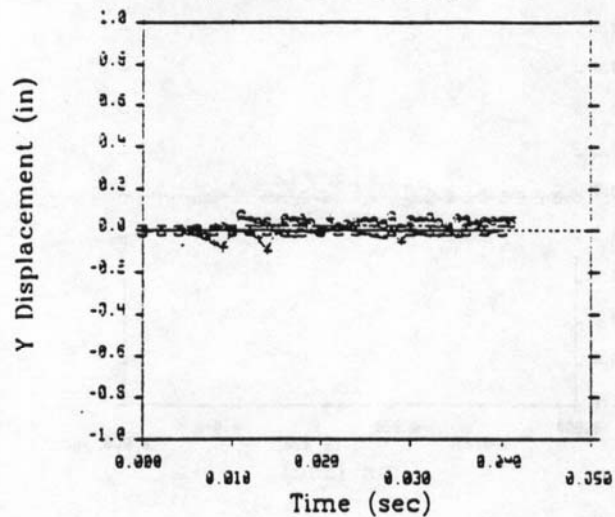
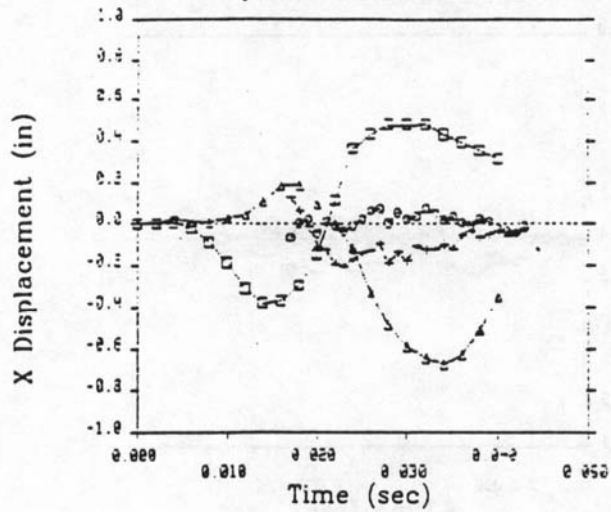


Figure 5: No Slip Physical and Finite Element  
Y Boundary Displacement vs Time

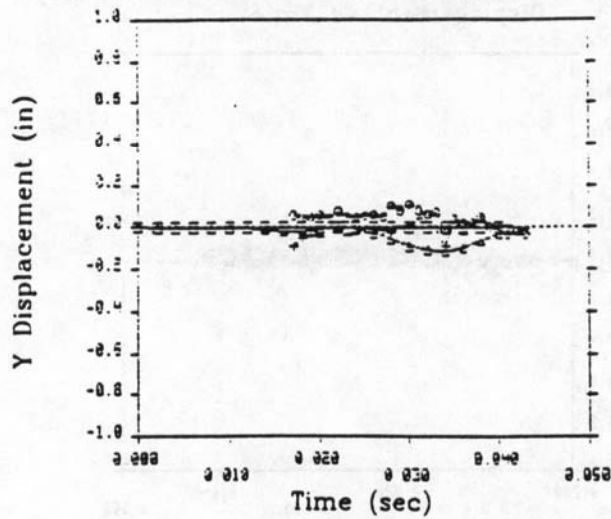
Slip Physical and Finite Element X Boundary  
Displacement vs Time



○ Physical Model  $r/R = 0$   
 □ Finite Element Model  $r/R = 0$   
 + Physical Model  $r/R = 1$   
 △ Finite Element Model  $r/R = 1$

Figure 6: Slip Physical and Finite Element  
X Boundary Displacement vs Time

Slip Physical and Finite Element Y Boundary  
Displacement vs Time



○ Physical Model  $r/R = 0$   
 □ Finite Element Model  $r/R = 0$   
 + Physical Model  $r/R = 1$   
 △ Finite Element Model  $r/R = 1$

Figure 7: Slip Physical and Finite Element  
Y Boundary Displacement vs Time

No Slip X Displacement at  $r/R = 0.25$  vs Time

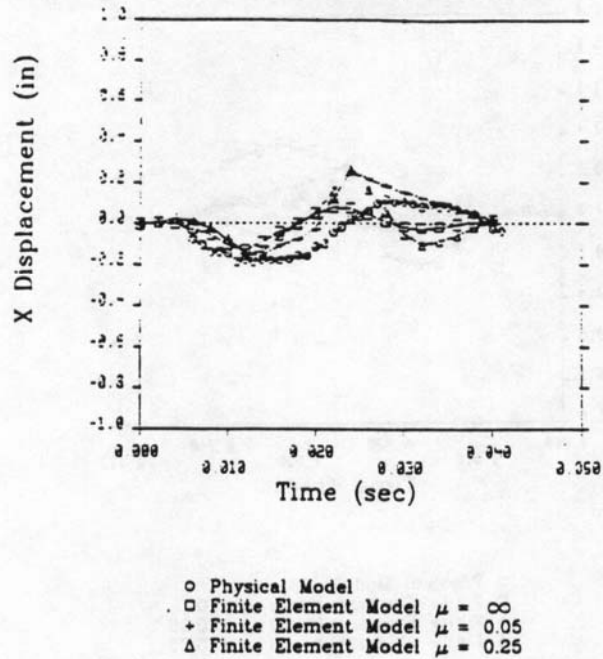


Figure 8: No Slip X Displacement at  $r/R = 0.25$  vs Time

No Slip X Displacement at  $r/R = 0.75$  vs Time

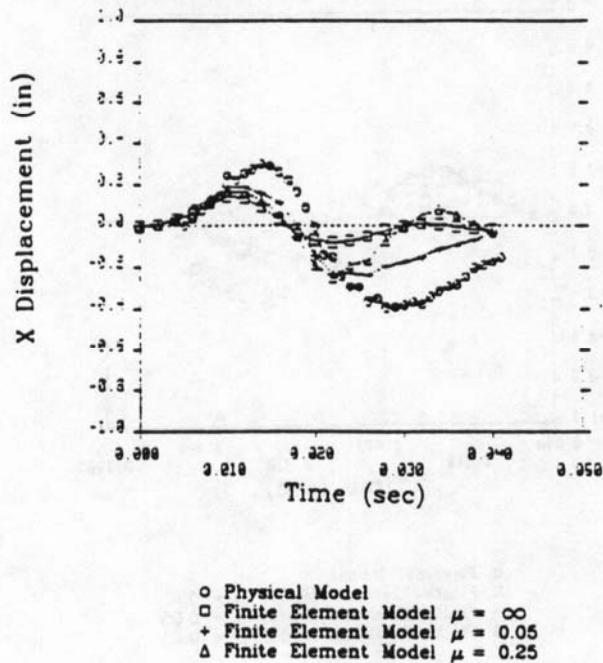


Figure 9: No Slip X Displacement at  $r/R = 0.75$  vs Time

Slip X Displacement at  $r/R = 0.25$  vs Time

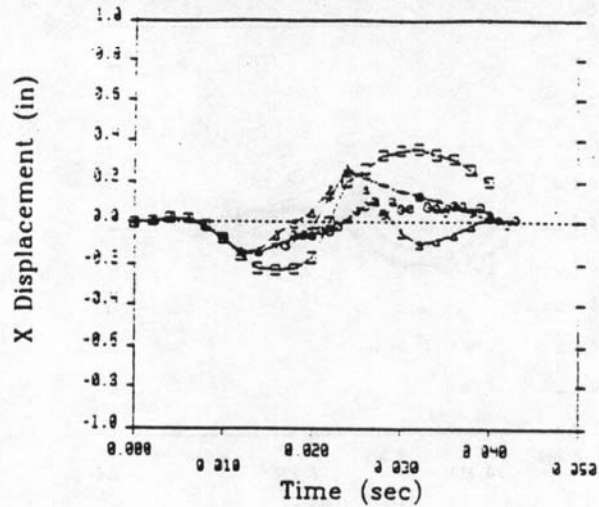


Figure 10: Slip X Displacement at  $r/R = 0.25$  vs Time

Slip X Displacement at  $r/R = 0.75$  vs Time

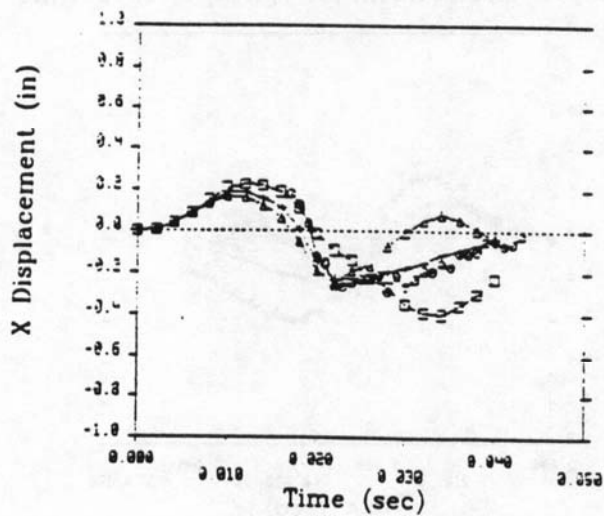


Figure 11: Slip X Displacement at  $r/R = 0.75$  vs Time



model: c4 30 8/13/88  
 TIME = 0.20000E-01  
 MAXIMUM PRINC STRAIN  
 (GREEN-ST. VENANT)  
 MIN= 0.735E-02 IN ELEMENT 1  
 MAX= 0.925E-02 IN ELEMENT 320

CONTOUR VALUES  
 A= 0.000E+00  
 B= 0.000E+00  
 C= 0.000E+00  
 D= 0.000E+00  
 E= 0.000E+00  
 F= 0.000E+00  
 G= 0.000E+00  
 H= 0.000E+00  
 I= 0.000E+00

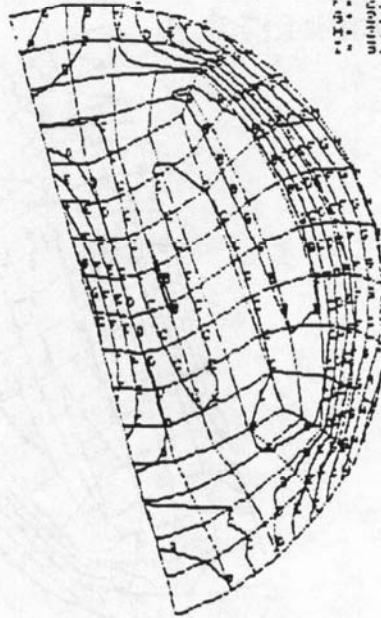


Figure 14: No Slip Finite Element Model  
 Green's Strains at 20 msec

model c5 (8/18/88)  
 TIME = 0.20000E-01  
 MAXIMUM PRINC STRAIN  
 (GREEN-ST. VENANT)  
 MIN= 0.126E-02 IN ELEMENT 122  
 MAX= 0.610E-02 IN ELEMENT 189

CONTOUR VALUES  
 A= 5.31E-02  
 B= 1.17E-01  
 C= 1.81E-01  
 D= 2.46E-01  
 E= 3.10E-01  
 F= 3.74E-01  
 G= 4.39E-01  
 H= 5.03E-01  
 I= 5.67E-01



Figure 15: Slip Finite Element Model  
 Green's Strains at 20 msec



model: c4 3D 8/10/88  
 TIME = 0.40000E-01  
 MAXIMUM PRINC STRAIN  
 (GREEN-ST. VENANT)  
 MIN= 0.220E-02 IN ELEMENT 304  
 MAX= 0.887E-01 IN ELEMENT 191

CONTOUR VALUES  
 I= 1.11E-01  
 H= 1.11E-01  
 G= 1.11E-01  
 F= 1.11E-01  
 E= 1.11E-01  
 D= 1.11E-01  
 C= 1.11E-01  
 B= 1.11E-01  
 A= 1.11E-01

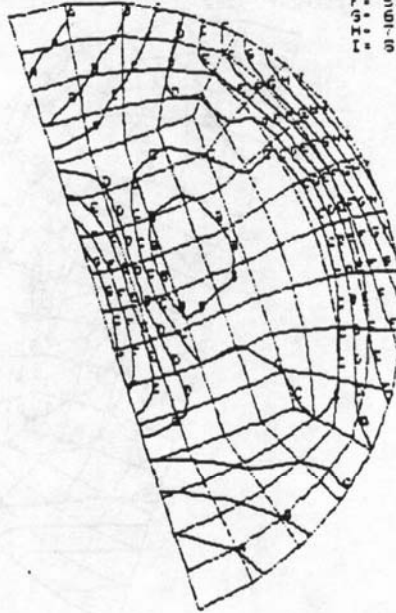


Figure 18: No Slip Finite Element Model  
 Green's Strains at 40 msec

model: c5 (8/10/88)  
 TIME = 0.40000E-01  
 MAXIMUM PRINC STRAIN  
 (GREEN-ST. VENANT)  
 MIN= 8.134E-01 IN ELEMENT 175  
 MAX= 8.443E-00 IN ELEMENT 355

CONTOUR VALUES  
 A= 4.95E-02  
 B= 9.41E-02  
 C= 1.39E-01  
 D= 1.83E-01  
 E= 2.28E-01  
 F= 2.73E-01  
 G= 3.17E-01  
 H= 3.62E-01  
 I= 4.07E-01

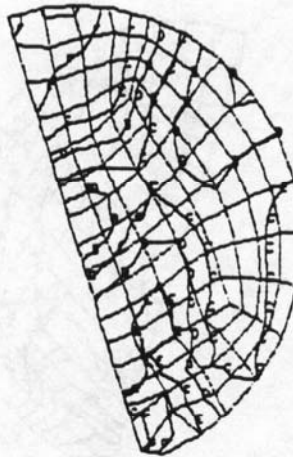


Figure 19: Slip Finite Element Model  
 Green's Strains at 40 msec

Maximum Principal Strain within Model vs Time

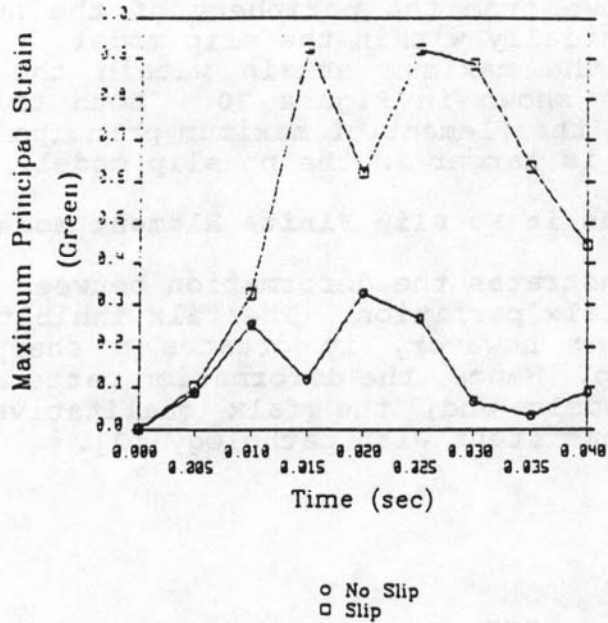


Figure 20: Maximum Principal Green's Strain within Finite Element Model vs Time

Strain in Element of Maximum Principal Strain vs Time

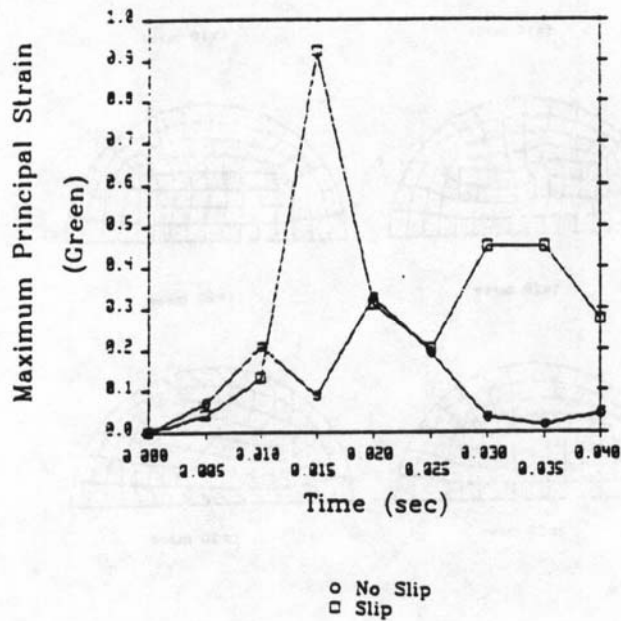


Figure 21: Green's Strain in Finite Element of Maximum Principal Strain vs Time

contour does not move from the periphery of the no slip model, but it does vary spatially within the slip model.

The value of the maximum strain within the models as a function of time is shown in Figure 20. Both this figure and Figure 21, strain in the element of maximum principal strain, show that Green's strain is larger in the no slip model.

#### Additional Partitions in No Slip Finite Element Model

Figure 22 demonstrates the deformation between a no slip FEM with and without a falx partition. The falx inhibits the overall motion of the brain; however, it creates a sharp deformation gradient near the tip. Hence, the deformation pattern is different between the two models and, the falx qualitatively generates results which are consistent with pathology [2].

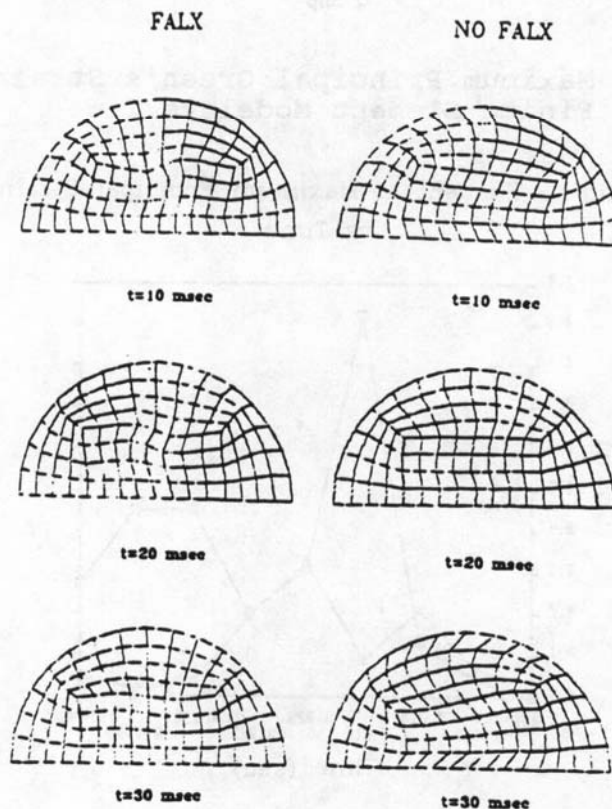


Figure 22: Finite Element Model Deformation With and Without Falx

## CONCLUSIONS

The current finite element model nodal displacements agree well with those of the University of Pennsylvania physical models when coefficients of friction are added into the interior-shell interface. These finite element models are then used to determine that the pure no slip condition yields larger values of Green's strain than the pure slip condition. Finally, it has been demonstrated that the addition of geometrically complexity will alter the deformation pattern within the model.

## REFERENCES

1. Thibault, L.E., et. al. Physical Model Experiments of the Brain Undergoing Dynamic Loading. Advances in Bioengineering. New York, New York, 1982.
2. Margulies, S.S. Biomechanics of Traumatic Coma in Primates. Ph.D. Thesis. University of Pennsylvania. 1987.
3. Hallquist, J.O., and Benson, D.J. DYNA3D USER'S MANUAL (Nonlinear Dynamic Analysis of Structures in Three Dimensions). Lawrence Livermore National Laboratory. 1987.

The present study is a continuation of the work of the author and his colleagues in the field of the dynamics of the motion of a rigid body. The results of the present study are presented in the form of a series of papers. The first paper is devoted to the study of the motion of a rigid body in a uniform gravitational field. The second paper is devoted to the study of the motion of a rigid body in a non-uniform gravitational field. The third paper is devoted to the study of the motion of a rigid body in a uniform magnetic field. The fourth paper is devoted to the study of the motion of a rigid body in a non-uniform magnetic field. The fifth paper is devoted to the study of the motion of a rigid body in a uniform electric field. The sixth paper is devoted to the study of the motion of a rigid body in a non-uniform electric field. The seventh paper is devoted to the study of the motion of a rigid body in a uniform electromagnetic field. The eighth paper is devoted to the study of the motion of a rigid body in a non-uniform electromagnetic field. The ninth paper is devoted to the study of the motion of a rigid body in a uniform gravitational and magnetic field. The tenth paper is devoted to the study of the motion of a rigid body in a non-uniform gravitational and magnetic field. The eleventh paper is devoted to the study of the motion of a rigid body in a uniform gravitational and electric field. The twelfth paper is devoted to the study of the motion of a rigid body in a non-uniform gravitational and electric field. The thirteenth paper is devoted to the study of the motion of a rigid body in a uniform gravitational, magnetic and electric field. The fourteenth paper is devoted to the study of the motion of a rigid body in a non-uniform gravitational, magnetic and electric field. The fifteenth paper is devoted to the study of the motion of a rigid body in a uniform gravitational, magnetic, electric and electromagnetic field. The sixteenth paper is devoted to the study of the motion of a rigid body in a non-uniform gravitational, magnetic, electric and electromagnetic field.

Author: [Name], [Address], [City], [State], [Country].

Received: [Date].

Published: [Date].

DISCUSSION

PAPER: Boundary Conditions in Head Injury. Finite Element Modeling

SPEAKER: Cathy Galbriath, DOT, Transportation Research Center

No Questions

SECRET

1. The purpose of this document is to provide information regarding the activities of the [redacted] in the [redacted] area.

2. The information contained herein is classified as [redacted] and is intended for the use of [redacted] only.

3. This document is to be controlled in accordance with the [redacted] policy.